Why do classifier accuracies show linear trends under distribution shift?

Horia Mania Suvrit Sra

Department of Electrical Engineering and Computer Science

Massachusetts Institute of Technology

{hmania, suvrit}@mit.edu

December 30, 2020

Abstract

Several recent studies observed that when classification models are evaluated on two different data distributions, the models' accuracies on one distribution are approximately a linear function of their accuracies on another distribution. We offer an explanation for these observations based on two assumptions that can be assessed empirically: (1) certain events have similar probabilities under the two distributions; (2) the probability that a lower accuracy model correctly classifies a data point sampled from one distribution when a higher accuracy model classifies it incorrectly is small.

1 Introduction

To determine whether the machine learning community has overfit to the test sets of popular datasets, several studies attempt to replicate the original data collection pipelines and then evaluate models on newly collected data [14, 15, 16, 22]. While these studies find no overfitting, some of them inadvertently induce a shift between the distributions of the original and new test sets that leads to a drop in model performance. Recht et al. [15] observe accuracy drops of 3% - 15% on CIFAR-10 [12] and of 11% - 14% on ImageNet [4]. Their observations are summarized in Figure 1, from which one can also notice a surprising pattern. The accuracies measured on the new data are approximately a linear function of the accuracies measured on the original data, a phenomenon that has also been observed on question-answering data [14] and other variants of ImageNet [1, 21]. These observations raise the following natural questions:

Why are classification models approximately collinear when evaluated on two data distributions?

When can one expect this phenomenon to occur?

Answers to these questions might lead to insights into improving model robustness because training a model robust to distribution shift would mean training a model that is not collinear with models developed previously. Therefore, to build robust models it would be helpful to first understand why the models available today are approximately collinear.

Model robustness is essential for deploying machine learning in real world applications, yet models available today are brittle. Recht et al. [15] show that distribution shift that leads to a large drop in accuracy can occur even in a controlled experiment, when one strives to replicate a data collection pipeline. Moreover, performance deterioration worsens when using data sources different from those used for model

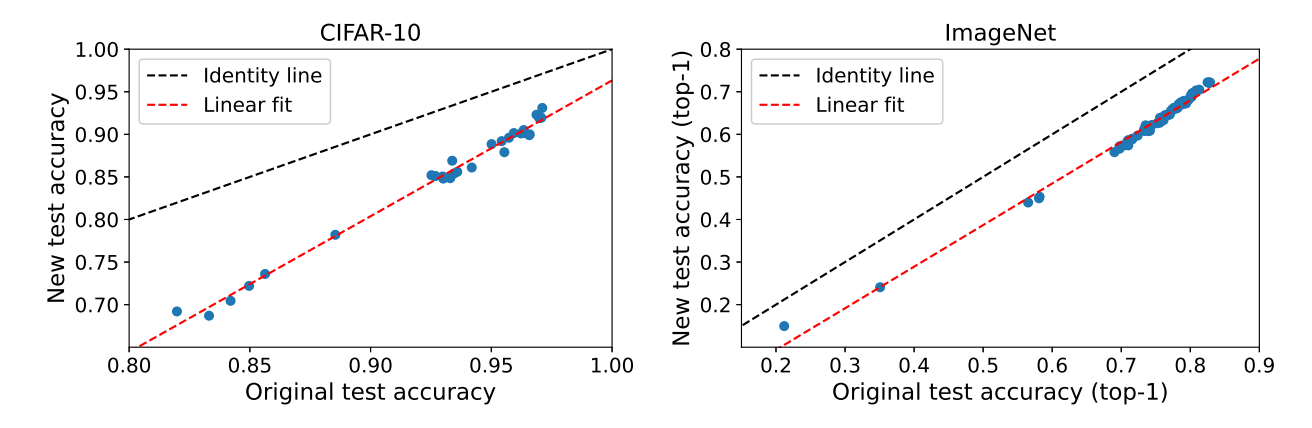


Figure 1: These two figures summarize the findings of Recht et al. [15]. The blue points in the left plot represent 30 CIFAR-10 models evaluated on both the original test set and a new test set, known as CIFAR-10.1. The right plot shows 66 ImageNet models evaluated on both the original validation set and a new test set, known as ImageNetV2. For more examples of distributions shifts, with and without linear trends, one should visit robustness.imagenetv2.org to visualize the testbed developed by Taori et al. [21].

development [1, 14] (e.g., using question-answering prompts from Reddit comments instead of Wikipedia articles). Therefore, if we hope to build machine learning systems that perform reliably on data from multiple sources, we must train models that are robust to some amount of distribution shift. In other words, we must find models that fall on the identity lines (black dashed lines) in Figure 1.

A growing body of work is trying to build robust models [2, 3, 5, 9, 17, 18, 20], but currently there are no models with non-trivial accuracy that are robust to the distribution shifts introduced by Recht et al. [15] on CIFAR-10 and ImageNet [21]. We know that it is possible to achieve the same accuracy on ImageNetV2 and ImageNet since human labelers are capable of this feat [19]. We hope that understanding when and why are models approximately collinear would inform future work on robust machine learning.

We answer these questions by starting with two premises that can be verified on ImageNet and CIFAR-10. As it is to be expected, we make an assumption on the size of the distribution shift. In particular, given two data distributions, we assume that certain events have similar probabilities under the two distributions. This assumption cannot be so stringent as to not permit an accuracy drop between the two distributions, in which case another assumption is needed in order to guarantee collinearity. Inspired by the work of Mania et al. [13] on model similarity, we also assume that given two models the probability that the lower accuracy model classifies a data point correctly while the higher accuracy model classifies it incorrectly is small. In other words, we assume that high accuracy models dominate low accuracy models, i.e., they correctly classify most of the data points correctly classified by the low accuracy models. Both of our assumptions are satisfied by ImageNet and CIFAR-10 models.

Given these two assumptions we show that any three models are almost collinear when their accuracies measured on one distribution are plotted as a function of their accuracies on the other distribution. We also discuss refinements of our analysis that explain why a probit axis scaling leads to a better linear fit for ImageNet models, as observed by Recht et al. [15].

2 Problem statement

Let $\mathcal X$ be a covariate space and $\mathcal Y$ a discrete label space. Let $\mathbb P$ and $\mathbb Q$ be two probability distributions on $\mathcal X \times \mathcal Y$. Also, suppose we have a set of models f_1, f_2, \ldots, f_h that map $\mathcal X$ to $\mathcal Y$. We are interested in the accuracies $\mu_i := \mathbb E_{\mathbb P} \mathbb 1(f_i(x) = y)$ and $\tilde \mu_i := \mathbb E_{\mathbb Q} \mathbb 1(f_i(x) = y)$, where the expectations are taken with respect to the data point (x,y), which belongs to $\mathcal X \times \mathcal Y$, and is distributed according to $\mathbb P$ and $\mathbb Q$, respectively. Given this notation, our main goal is to show that $\{(\mu_i, \tilde \mu_i)\}_{i=1}^h$ are approximately collinear, which can be formulated more precisely as follows:

Problem 1. Under a set of assumptions, we wish to show that there exist $\alpha, \beta \in \mathbb{R}$ such that $\tilde{\mu}_i \approx \alpha \mu_i + \beta$ for all $i \in \{1, 2, ..., h\}$.

We make two assumptions. Firstly, to upper bound the distance between \mathbb{Q} and \mathbb{P} we assume that $\mathbb{Q}(A)$ is close to $\mathbb{P}(A)$ for a collection of events A. To state the assumption precisely, for a model f_i , we denote by A_i^+ the subset of $\mathcal{X} \times \mathcal{Y}$ on which f_i is correct and by A_i^- the subset on which f_i is incorrect.

Assumption 1. There exist non-negative real numbers δ_1 , δ_2 , ν_1 , ν_2 such that for all distinct $i, j, k \in \{1, 2, ..., h\}$ and $(\varepsilon_i, \varepsilon_j, \varepsilon_k) \in \{-, +\}^3$, different from (-, -, -) and (+, +, +), we have

$$-\nu_{1} + (1 - \delta_{1}) \mathbb{P}(A_{i}^{\varepsilon_{i}} \cap A_{j}^{\varepsilon_{j}} \cap A_{k}^{\varepsilon_{k}}) \leq \mathbb{Q}(A_{i}^{\varepsilon_{i}} \cap A_{j}^{\varepsilon_{j}} \cap A_{k}^{\varepsilon_{k}})$$

$$\leq \nu_{2} + (1 + \delta_{2}) \mathbb{P}(A_{i}^{\varepsilon_{i}} \cap A_{j}^{\varepsilon_{j}} \cap A_{k}^{\varepsilon_{k}}). \tag{1}$$

In Section 3 we discuss this assumption in detail. For now we make a few remarks. Assumption 1 only imposes constraints on the probabilities $\mathbb{Q}(A)$ of $6\binom{h}{3}$ events A, which means that the distance between \mathbb{Q} and \mathbb{P} is allowed to be large when measured using traditional distances such as TV or KL. We also want to stress that the linear form of (1) is not essential and it does not imply a linear fit by itself. Coincidentally, inequalities of the form $\mathbb{Q}(A) \leq \nu + (1+\delta)\mathbb{P}(A)$ are used in differential privacy to compare the distributions of outputs of a randomized algorithm applied to two different databases [6, 7, 8].

Since Assumption 1 alone does not ensure models are approximately collinear (unless the parameters δ and ν are much smaller than the values we observe in practice), we must make an additional assumption. Mania et al. [13] observe that the predictions of image classification models are highly correlated (given two models the probability that they are both correct or incorrect when classifying a data point is high). Inspired by this observation, we make the following related assumption.

Assumption 2. For all models f_i and f_j with $\mu_i \leq \mu_j$ the probability $\mathbb{P}(\{f_i(x) = y\} \cap \{f_j(x) \neq y\}) \leq \zeta$.

We discuss this assumption in Section 4, where we show that most probabilities $\mathbb{P}(\{f_i(x)=y\}\cap\{f_j(x)\neq y\})$ for CIFAR-10 and ImageNet models are less than 0.05. When the set of models $\{f_i\}_{i=1}^h$ satisfies Assumption 2 with $\zeta=0$ we say that it is *ordered*. Also, if f_i and f_j are two models such that $\mu_i \leq \mu_j$ and $\mathbb{P}(\{f_i(x)=y\}\cap\{f_j(x)\neq y\})=0$, we say that f_j dominates f_i . More generally, we call $\mathbb{P}(\{f_i(x)=y\}\cap\{f_j(x)\neq y\})$ the dominance probability.

The main idea of our solution to Problem 1 is to look at any three models f_i , f_j , and f_k with $\mu_i \le \mu_j \le \mu_k$ and to consider the line ℓ determined by the points $(\mu_i, \tilde{\mu}_i)$ and $(\mu_k, \tilde{\mu}_k)$. Then, we upper bound the residual from $(\mu_j, \tilde{\mu}_j)$ to the line ℓ , i.e. we upper bound $|\ell(\mu_j) - \tilde{\mu}_j|$. The next result encapsulates our analysis when the set of models is ordered.

Proposition 1. Given an ordered set of models $f_1, f_2, ..., f_h$ and two probability distributions \mathbb{P} and \mathbb{Q} that satisfy Assumption 1, for any three models f_i, f_j, f_k with $\mu_i \leq \mu_j \leq \mu_k$ we have

$$|\ell(\mu_j) - \tilde{\mu}_j| \le \frac{\delta_1 + \delta_2}{2} \frac{2(\mu_k - \mu_j)(\mu_j - \mu_i)}{\mu_k - \mu_i} + \max\{\nu_1, \nu_2\} + \left(1 + \frac{\max\{\mu_k - \mu_j, \mu_j - \mu_i\}}{\mu_k - \mu_i}\right) \nu_2, \quad (2)$$

where ℓ is the line defined by the points $(\mu_i, \tilde{\mu}_i)$ and $(\mu_k, \tilde{\mu}_k)$.

Note that the second factor in the first term of (2) is the harmonic mean of $\mu_k - \mu_j$ and $\mu_j - \mu_i$. To gain intuition about this bound, Figure 2a depicts our guarantee for three ordered models when $\delta_1 = \delta_2 = 0.2$ and $\nu_1 = \nu_2 = 0$. More concretely, we consider two hypothetical models f_i and f_j with $(\mu_i, \tilde{\mu}_i) = (0.4, 0.3)$ and $(\mu_k, \tilde{\mu}_k) = (0.8, 0.7)$. Then, Proposition 1 guarantees that any other model f_j with $0.3 \le \mu_j \le 0.8$ that dominates f_i and is dominated by f_k must lie in between the dashed red curves shown in Figure 2a. Therefore, if we were to draw the line defined by the two blue points, all other models would lie close to it.

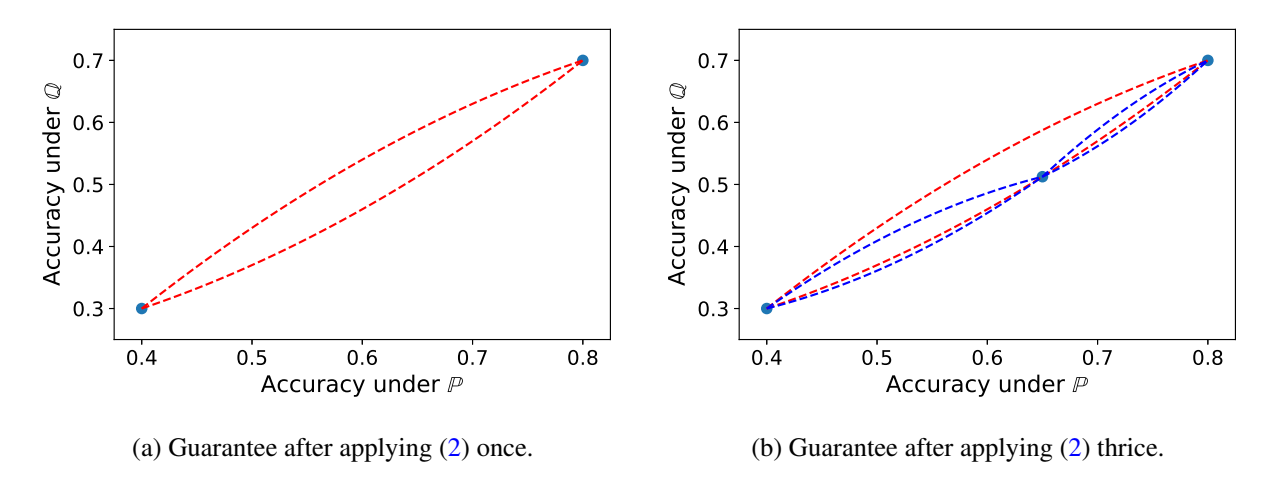


Figure 2: A depiction of the bound (2) when applied to a hypothetical distribution shift that satisfies Assumption 1 with $\delta_1 = \delta_2 = 0.2$ and $\nu_1 = \nu_2 = 0$, and to a hypothetical set of models that is ordered. Any other model would have to lie in between the red and blue dashed curves.

Moreover, the bound (2) applies to any subset of three models. Figure 2b shows what kind of guarantee we can obtain when we take advantage of this fact. Suppose f_j is the middle blue point shown in Figure 2b. Then, by applying (2) two more times we see that a fourth model would have to lie not only between the two red dashed lines, but also in one of the two areas delineated by the blue dashed curves. Therefore, in cases when a linear fit produces residuals that are larger than desired, one should expect to see a much better fit when using piecewise linear regression with a small number of pieces. We come back to this point in Section 5.3, when we discuss why using probit scaling for plotting the ImageNetV2 accuracies as a function of ImageNet accuracies improves the linear fit. One can also see from Figure 2b that once we can guarantee that any three points are approximately collinear, it follows that all points are approximately collinear.

3 The size of distribution shift

In this section we aim to motivate and interpret our assumption on the distribution shift between \mathbb{P} and \mathbb{Q} . Of course, for any distributions \mathbb{P} and \mathbb{Q} there exist parameters δ_1 , δ_2 , ν_1 and ν_2 such that Assumption 1

holds. However, this trivial point is not sufficient to justify our assumption. It is a good sign that Kpotufe and Martinet [11] used a similar assumption to analyze the sample complexity of transfer learning. They assume $\mathbb{Q}(A) \leq (1+\delta)\mathbb{P}(A)$ where the events A are balls centered at different x's.

The main advantage of (1) is that it must hold only for a finite number of subsets $A \subset \mathcal{X} \times \mathcal{Y}$ in order for our analysis to go through. Moreover, for the required events A, we can estimate $\mathbb{P}(A)$ and $\mathbb{Q}(A)$ on CIFAR-10 and ImageNet and find δ_1 , δ_2 , ν_1 , and ν_2 such that (1) holds. Therefore, we can validate our assumption empirically.

For any data point $(x,y) \in \mathcal{X} \times \mathcal{Y}$ a model can either classify it correctly or incorrectly. Hence, given three models there are 8 possible correctness outcomes. Assumption 1 imposes probability constraints on only 6 of the corresponding events. To understand why we do not need to impose any restrictions on $\mathbb{Q}(A_i^- \cap A_j^- \cap A_k^-)$ and $\mathbb{Q}(A_i^+ \cap A_j^+ \cap A_k^+)$, note that changes in these two probabilities would move the three points $(\mu_i, \tilde{\mu}_i)$, $(\mu_j, \tilde{\mu}_j)$, and $(\mu_k, \tilde{\mu}_k)$ up or down equally. Therefore, the two probabilities would have no effect on how closely to a line the three points lie.

Refinements of Assumption 1. In some situations we might want to refine Assumption 1 to get tighter guarantees. Our analysis, presented in Section 5, shows that any three models are approximately collinear. Suppose we are given four models f_1 , f_2 , f_3 , and f_4 and suppose (1) is satisfied by the events defined by (f_1, f_2, f_4) and (f_1, f_3, f_4) . Then, we can show that f_2 and f_3 lie close to the line defined by f_1 and f_4 , without needing the events defined by (f_1, f_2, f_3) and (f_2, f_3, f_4) to satisfy (1). Therefore, in certain situations we can still guarantee that all models are approximately collinear without requiring (1) to hold for all $6\binom{h}{3}$ events introduced in Assumption 1.

We can also refine Assumption 1 as follows. We can have two sets of parameters $(\delta_1, \delta_2, \nu_1, \nu_2)$, one for events that have small probability (e.g. less than 0.05) under $\mathbb P$ and one for events with larger probability under $\mathbb P$. Having larger δ_1 and δ_2 for events A with $\mathbb P(A) \leq 0.05$ would not impact the results significantly because $|\mathbb Q(A) - \mathbb P(A)|$ would still be small in this case. More generally, our analysis can be carried out with bounds of the form

$$-g_1(\mathbb{P}(A)) \le \mathbb{Q}(A) - \mathbb{P}(A) \le g_2(\mathbb{P}(A))$$

for some non-negative functions g_1 , g_2 . Such a notion of closeness is important in the case of CIFAR-10 since for this dataset the linear bounds on $\mathbb{Q}(A)$ would require large δ_2 and ν_2 although $|\mathbb{Q}(A) - \mathbb{P}(A)|$ is small for all events A of interest. We discuss this point further in Appendix A.

ImageNetV2 and **ImageNet satisfy Assumption 1.** We study h = 66 ImageNet models that were collated and evaluated by Recht et al. [15] ¹. We would like to find parameters δ_1 , δ_2 , ν_1 , and ν_2 such that (1) holds for 274,560 events when the probabilities are evaluated under the ImageNetV2 and ImageNet distributions.

We evaluate empirically the probabilities of the 274,560 events on the two datasets. Of course, the empirical estimates of these probabilities suffer from some estimation error, especially given the large number of estimates we require. Nonetheless, this exercise gives us an understanding of what are reasonable δ_1 , δ_2 , ν_1 , and ν_2 for the two datasets.

The blue points shown in Figure 3a represent probabilities of the 274,560 events defined by the triplets $\{f_i, f_j, f_k\}$. As can be shown from Figure 3a, all blue points lie in a wedge defined by two lines, with slopes 0.69 and 1.38 and with y-axis intercepts -0.005 and 0.008 respectively. Therefore, this empirical evaluation

¹Recht et al. [15] provide 67 models, but we take out one of the three Fisher vector models because, although it is approximately collinear with the rest of the models, a few of the events it induces are outliers in relation to Assumption 1.

suggests that ImageNet and ImageNetV2 satisfy our assumption with $\delta_1=0.31,\,\delta_2=0.38,\,\nu_1=0.005,$ and $\nu_2=0.008.$

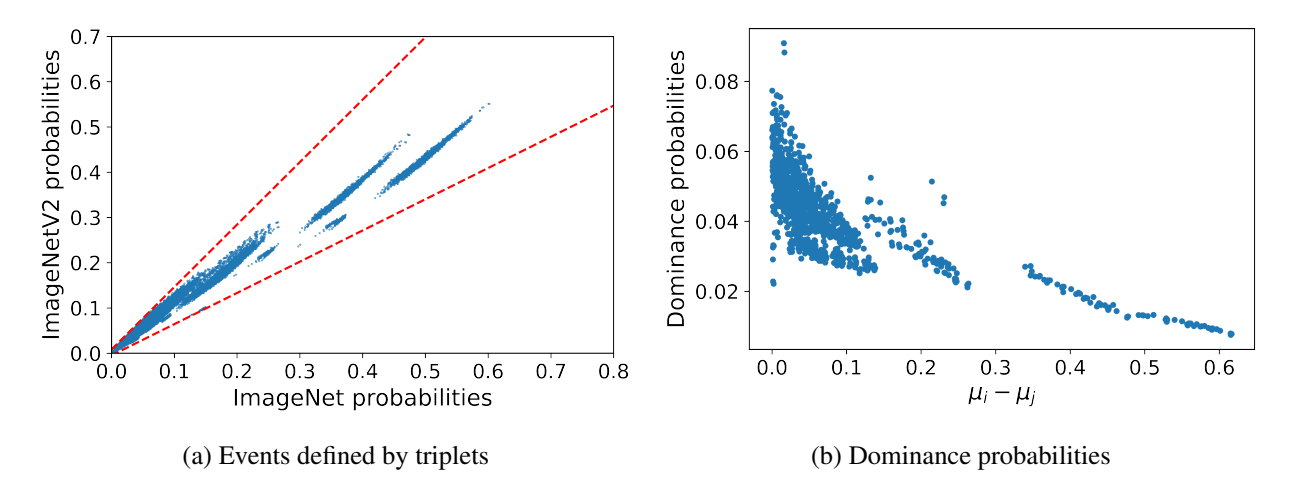


Figure 3: Figure 3a shows 274,560 blue points representing the probabilities of the events $A_i^{\varepsilon_i} \cap A_j^{\varepsilon_j} \cap A_k^{\varepsilon_k}$. The red dotted lines are upper and lower bounds on the probabilities according to ImageNetV2, as in (1), with parameters: $\delta_1 = 0.31$, $\delta_2 = 0.38$, $\nu_1 = 0.005$, and $\nu_2 = 0.008$. Figure 3b shows the probabilities of the events $A_i^+ \cap A_j^-$ for all pairs of models with $\mu_i < \mu_j$ (i.e., the events on which a worse model is correct, but a better model is incorrect).

Following the refinement strategies described above, if we only require 95% of the 274,560 points to lie inside the wedge, we can choose $\delta_1=0$, $\delta_2=0.25$, $\nu_1=0.005$, and $\nu_2=0.005$. Therefore, the vast majority of points lie in a much smaller wedge than the worst case wedge considered previously. This observation is useful in Section 5.3 when we discuss the linear fit in probit domain.

4 Model dominance

Mania et al. [13] observe that models trained on CIFAR-10 and on ImageNet make similar predictions and used this observation to show that one can re-use test sets more times than previously expected without overfitting. More concretely, they define the similarity between two models f_i and f_j to be

$$\mathbb{P}(\mathbb{1}\{f_i(x) = y\} = \mathbb{1}(f_i(x) = y)).$$

If two models were making mistakes independently of each other, one would expect the similarity to be $\mu_i\mu_j + (1 - \mu_i)(1 - \mu_j)$. However, on ImageNet, Mania et al. [13] observe model similarities that are approximately 0.25 higher than this quantity.

Model similarity is a bit difficult to work with for our purposes because whether a certain similarity value is high or not depends on the accuracy of the models, and in this work we consider models that are anywhere between 21% and 83% accurate.

Instead, we work with a related quantity. Given two models f_i and f_j with $\mu_i \leq \mu_j$ we consider the probability that f_i classifies a data point correctly while f_j does not:

$$\mathbb{P}(\{f_i(x) = y\} \cap \{f_j(x) \neq y\}). \tag{3}$$

We say that f_j dominates f_i when this probability is zero and we say that f_j approximately dominates f_i when this probability is close to zero (e.g. less than 0.05). We refer to the probabilities $\mathbb{P}(\{f_i(x) = y\} \cap \{f_j(x) \neq y\})$ as dominance probabilities.

In Figure 3b we plot the dominance probabilities (3) for $\binom{66}{2}$ pairs of ImageNet models as a function of the difference between their accuracies. Two things are worth nothing. First of all, all the dominance probabilities are less than 0.09 with most of them being less than 0.05. Moreover, we note that the dominance probabilities decrease as the difference in accuracy between the models increases. Therefore, on ImageNet it seems that the more accurate a model is the more it dominates lower accuracy models (i.e., it is less likely that the low accuracy model correctly classifies a data point when the high accuracy model classifies it incorrectly).

In the next section we first analyze the case when the set of models $f_1, f_2, ..., f_h$ is ordered (i.e., all dominance probabilities are zero) in order to clarify the main idea of our answer to Problem 1. Then, we discuss what happens when the dominance probabilities are small, as informed by Figure 3b.

5 Main arguments

In Section 5.1 we present the crux of our analysis under the simplifying assumption that the set of models f_1 , f_2, \ldots, f_h is ordered. Then, in Section 5.2 we discuss the general case, in which the dominance probabilities are small (less than 0.05), but not necessarily zero.

5.1 Linear fit for an ordered set of models

As a reminder, the set of models $f_1, f_2, ..., f_h$ is ordered if $\mathbb{P}(\{f_i(x) = y\} \cap \{f_j(x) \neq y\}) = 0$ for all pairs of models f_i and f_j with $\mu_i \leq \mu_j$.

Now, let us consider three models f_1 , f_2 , and f_3 with $\mu_1 \leq \mu_2 \leq \mu_3$. Also, let ℓ be the line between the points $(\mu_1, \tilde{\mu}_1)$ and $(\mu_3, \tilde{\mu}_3)$. Then, we upper bound the residual from $(\mu_2, \tilde{\mu}_2)$ to ℓ in the vertical direction (whenever we refer to a residual, it is measured along the y-axis). To express this residual recall that $A_1^+ = \{f_1(x) = y\}$ and $A_1^- = \{f_1(x) \neq y\}$ and define the quantities:

$$p_{123} = \mathbb{P}(A_1^+ \cap A_2^+ \cap A_3^+), \quad p_{23} = \mathbb{P}(A_1^- \cap A_2^+ \cap A_3^+), \quad p_3 = \mathbb{P}(A_1^- \cap A_2^- \cap A_3^+).$$

In plain language, p_{123} is the probability that all three models f_1 , f_2 , and f_3 classify a data point sampled from \mathbb{P} correctly. The term p_{23} is the probability that models f_2 and f_3 classify a data point sampled from \mathbb{P} correctly while f_1 classifies it incorrectly. By now it should be clear what p_1 represents. In the next section we also need to consider the probabilities:

$$p_1 = \mathbb{P}(A_1^+ \cap A_2^- \cap A_3^-), \quad p_{12} = \mathbb{P}(A_1^+ \cap A_2^+ \cap A_3^-),$$
$$p_2 = \mathbb{P}(A_1^- \cap A_2^+ \cap A_3^-), \quad p_{13} = \mathbb{P}(A_1^+ \cap A_2^- \cap A_3^+).$$

When the set of models is ordered these four probabilities are zero. Therefore, under the ordering assumption, we have

$$\mu_1 = p_{123}, \quad \mu_2 = p_{123} + p_{23}, \quad \mu_3 = p_{123} + p_{23} + p_3.$$
 (4)

We use q_{123} , q_{12} , q_1 and so on to denote the analogous probabilities under the distribution \mathbb{Q} . Note that although p_1 is zero, q_1 can be nonzero. When Assumption 1 and Assumption 2 with $\zeta = 0$ hold, we know that q_1, q_2, q_{12} , and q_{13} are at most ν_2 .

Now, the line ℓ between $(\mu_3, \tilde{\mu}_3)$ and $(\mu_1, \tilde{\mu}_1)$ is defined by the equation:

$$\ell(\mu) = \frac{\tilde{\mu}_3 - \tilde{\mu}_1}{\mu_3 - \mu_1} (\mu - \mu_1) + \tilde{\mu}_1$$

$$= \frac{q_{23} + q_3 - q_1 - q_{12}}{p_{23} + p_3} (\mu - p_{123}) + q_{123} + q_{12} + q_{13} + q_1.$$

Therefore, the residual r from $(\mu_2, \tilde{\mu}_2)$ to ℓ can be easily expressed:

$$r := \left| \frac{q_{23} + q_3 - q_1 - q_{12}}{p_{23} + p_3} p_{23} + q_{13} + q_1 - q_{23} - q_2 \right|$$

$$\leq \left| \frac{q_3 p_{23} - p_3 q_{23}}{p_{23} + p_3} \right| + \left| \frac{p_3}{p_3 + p_{23}} q_1 - \frac{p_{23}}{p_3 + p_{23}} q_{12} + q_{13} - q_2 \right|$$
(5)

When \mathbb{P} and \mathbb{Q} satisfy Assumption 1 we know that $0 \leq q_1, q_{13}, q_2, q_{12} \leq \nu_2$ and

$$-\nu_1 + (1 - \delta_1)p_3 \le q_3 \le (1 + \delta_2)p_3 + \nu_2$$

$$-\nu_1 + (1 - \delta_1)p_{23} \le q_{23} \le (1 + \delta_2)p_{23} + \nu_2.$$

Using these bounds in (5) immediately yields our main result.

Proposition 1. Given an ordered set of models $f_1, f_2, ..., f_h$ and two probability distributions \mathbb{P} and \mathbb{Q} that satisfy Assumption 1, for any three models f_i, f_j, f_k with $\mu_i \leq \mu_j \leq \mu_k$ we have

$$|\ell(\mu_j) - \tilde{\mu}_j| \le \frac{\delta_1 + \delta_2}{2} \frac{2(\mu_k - \mu_j)(\mu_j - \mu_i)}{\mu_k - \mu_i} + \max\{\nu_1, \nu_2\} + \left(1 + \frac{\max\{\mu_k - \mu_j, \mu_j - \mu_i\}}{\mu_k - \mu_i}\right) \nu_2, \quad (2)$$

where ℓ is the line defined by the points $(\mu_i, \tilde{\mu}_i)$ and $(\mu_k, \tilde{\mu}_k)$.

We can improve this result by a factor of 2. For convenience, let us denote by A, B, and C the three points $(\mu_1, \tilde{\mu}_1)$, $(\mu_2, \tilde{\mu}_2)$, and $(\mu_3, \tilde{\mu}_3)$. Now, instead of looking at the line ℓ that passes through A and C let us look at the line ℓ' that is defined by the middles points of the segments AB and BC. One can easily see that the residual between B and the line ℓ' is upper bounded by:

$$r' \le \frac{p_3 p_{23}}{p_3 + p_{23}} \frac{\delta_1 + \delta_2}{2} + \frac{1}{2} \max\{\nu_1, \nu_2\} + \frac{1}{2} \left(1 + \frac{\max\{p_3, p_{23}\}}{p_3 + p_{23}} \right) \nu_2, \tag{6}$$

gaining a factor of 2 over (2).

Proposition 1 is the core of our answer to Problem 1. It shows that any three models must be approximately collinear when Assumption 1 holds and the set of models is ordered. Moreover, it is intuitive that when any three models are approximately collinear, all models must be approximately collinear. In the next corollary we show how this argument can be made precise. The constant 25/64 in Corollary 1 can be improved.

Corollary 1. If the set of models $\{f_i\}_{i=1}^h$ is ordered and the distributions \mathbb{P} and \mathbb{Q} satisfy Assumption 1 with $\nu_1 = \nu_2 = 0$, there exists a line ℓ such that the residual from any point $(\mu_i, \tilde{\mu}_i)$ to it is at most

$$\frac{25}{64}(\mu_h - \mu_1)\frac{\delta_1 + \delta_2}{2} + 3\max\{\nu_1, \nu_2\}. \tag{7}$$

Proof. Let $A = (\mu_1, \tilde{\mu}_1)$ and $C = (\mu_h, \tilde{\mu}_h)$, and let $B = (\mu_i, \tilde{\mu}_i)$ be the point that has the largest residual from the line AC. Without loss of generality we assume that B is below or on the line AC. Then, there are two cases: all other models fall on or below the line AC, or there exists at least a point above the line AC.

The first case is immediately resolved by applying Proposition 1 to upper bound the residual r_B of B from the line AC. Then, we can choose ℓ to be the line that passes through the middle of the segments AB and BC. For this choice of ℓ the residual of any other point in our collection is upper bounded by $r_B/2$ because B has the largest residual and all other points lie on or below AC. The conclusion follows because the harmonic mean of two numbers with a constant sum is maximized when the two numbers are equal.

For the second case, let $D=(\mu_j,\tilde{\mu}_j)$ a point above the line AC with the largest residual from AC. We can assume that $\mu_1<\mu_j<\mu_i$. Let r_B and r_D be B's and D's residuals from the line AC. By our extremal choices of B and D we know that if we consider the lines parallel to AC that pass through B and D respectively, we are guaranteed that all other points lie between them. Therefore, we can choose a line parallel to AC that has residual at most $(r_D+r_B)/2$ from all points.

Hence, we are left to upper bound r_B and r_D . From Proposition 1 we know that

$$r_B \le \frac{2(\mu_h - \mu_i)(\mu_1 - \mu_i)}{\mu_h - \mu_1} \frac{\delta_1 + \delta_2}{2} + 3 \max\{\nu_1, \nu_2\}.$$
(8)

Since D is above the line AC, if we define by r'_D the residual from D to BC, we have $r_D \leq r'_D$. Then, from Proposition 1 we know that

$$r_D \le r_D' \le \frac{2(\mu_i - \mu_j)(\mu_j - \mu_1)}{\mu_i - \mu_1} \frac{\delta_1 + \delta_2}{2} + 3 \max\{\nu_1, \nu_2\}. \tag{9}$$

Let $c := \mu_j - \mu_1$, $b := \mu_i - \mu_j$, and $a := \mu_h - \mu_i$. Then, putting together (8) and (9) we find

$$r_B + r_D \le \frac{2bc}{b+c} \frac{\delta_1 + \delta_2}{2} + \frac{2a(b+c)}{a+b+c} \frac{\delta_1 + \delta_2}{2} + 6 \max\{\nu_1, \nu_2\}.$$

Now, we would like to understand how large can the right hand side be as a function of just δ_1 , δ_2 , ν_1 , ν_2 , and $\mu_h - \mu_1$. In order to do this we find the maximum of the right hand side with respect to a, b, and c under the constraints a, b, $c \ge 0$ and $a + b + c = \mu_h - \mu_1$. Using simple first order conditions, one can find that

$$r_B + r_D \le \frac{25}{32}(\mu_1 - \mu_h)\delta + 6\max\{\nu_1, \nu_2\}.$$

The result follows by taking ℓ to be the line parallel to AC with equal residuals to B and D.

5.2 Linear fit for an approximately ordered set of models

Now we discuss what happens when the set of models f_1 , f_2 , ... f_h is not ordered, i.e. when the dominance probabilities are allowed to be non-zero. Nonetheless, Figure 3b from Section 4 shows that these probabilities can be assumed to be small. In this section we assume they are at most 0.05.

We proceed as in the Section 5.1, using the same notation. We show that given three models f_1 , f_2 , f_3 the three points $(\mu_1, \tilde{\mu}_1)$, $(\mu_2, \tilde{\mu}_2)$, and $(\mu_3, \tilde{\mu}_3)$ are approximately collinear. Now, we have $\mu_1 = p_1 + p_{12} + p_{13} + p_{123}$, $\mu_2 = p_2 + p_{12} + p_{23} + p_{123}$, and $\mu_3 = p_3 + p_{13} + p_{23} + p_{123}$. Also, since the set of models is assumed to be approximately ordered, with $\mathbb{P}(\{f_i(x) = y\} \cap \{f_j(x) \neq y\}) \leq 0.05$ whenever $\mu_i \leq \mu_j$, we know that $p_1 + p_{12}$, $p_1 + p_{13}$, and $p_2 + p_{12}$ are at most 0.05.

As before, we compute the residual of the point $(\mu_2, \tilde{\mu}_2)$ from the line ℓ defined by $(\mu_1, \tilde{\mu}_1)$ and $(\mu_3, \tilde{\mu}_3)$. The equation parameterizing ℓ is

$$\ell(\mu) = \frac{\tilde{\mu}_3 - \tilde{\mu}_1}{\mu_3 - \mu_1} (\mu - \mu_1) + \tilde{\mu}_1.$$

Therefore, the residual r from $(\mu_2, \tilde{\mu}_2)$ to ℓ is

$$r = \left| \frac{q_3 + q_{23} - q_1 - q_{12}}{p_3 + p_{23} - p_1 - p_{12}} (\mu_2 - \mu_1) + \tilde{\mu}_1 - \tilde{\mu}_2 \right|$$

$$= \left| \frac{q_3 + q_{23} - q_1 - q_{12}}{p_3 + p_{23} - p_1 - p_{12}} (p_2 + p_{23} - p_1 - p_{13}) + q_1 + q_{13} - q_2 - q_{23} \right|$$
(10)

Numerical upper bound. Given our assumptions, to get the best possible upper bound on this residual, one would have to consider many cases, which are determined by the signs of various quantities inside the absolute value. Instead, we compute numerically an upper bound on (10).

Let us suppose $p_3=p_{23}=0.1$, which corresponds to $\mu_2-\mu_1\approx 0.1$ and $\mu_3-\mu_2\approx 0.1$. Our assumptions ensure that $p_1+p_{12},\,p_1+p_{13},\,p_2+p_{12}$ are at most 0.05 and that

$$\max\{0, -\nu_1 + (1 - \delta_1)p\} \le q \le \nu_2 + (1 + \delta_2)p,$$

for all $p \in \{p_1, p_2, p_3, p_{12}, p_{13}, p_{23}\}$ and corresponding q. Let us choose $\delta_1 = 0.31$, $\delta_2 = 0.38$, $\nu_1 = 0.005$, and $\nu_2 = 0.008$, which ensures that Assumption 1 is satisfied for ImageNetV2 vs ImageNet.

Then, with p_3 and p_{23} fixed to 0.1, we can grid over the allowed values for the remaining probabilities p and for the probabilities q and evaluate (10). This computation reveals that (10) is at most 0.083. Then, by shifting the line ℓ towards $(\mu_2, \tilde{\mu}_2)$, as in (6), we can half the residual. Therefore, in the case we are analyzing, there exists a line such that the residuals of the models f_1 , f_2 , and f_3 are at most 0.0415.

In Section 3 we saw that the choice $\delta_1 = 0.31$, $\delta_2 = 0.38$, $\nu_1 = 0.005$, and $\nu_2 = 0.008$ is conservative for ImageNetV2 vs ImageNet. Instead, we can choose $\delta_1 = 0.0$, $\delta_2 = 0.25$, $\nu_1 = 0.005$, and $\nu_2 = 0.005$ and then (1) is satisfied by 95% of the required events. With this choice of parameters, we can check numerically that (10) is at most 0.045, which means that there exists a line such that the residuals of the three models are most 0.0225. These numerical computations are further depicted in Figures 4a and 4b.

5.3 Discussion of probit axis scaling

Recht et al. [15] show that that using a probit axes scaling leads to a better linear fit for ImageNet models. Concretely, they fit a linear regression on the points $(\Phi^{-1}(\mu_i), \Phi^{-1}(\tilde{\mu}_i))$, where Φ is the CDF of the standard normal distribution, and observe a better linear fit than in Figure 1. The standard linear fit, shown on the right of Figure 1, produces a line with a maximum residual of 0.044 and a R^2 of 0.988. On the other hand, the linear fit in probit domain, shown as the red dashed curves in Figures 4a and 4b, yields a maximum residual of 0.01 and a R^2 of 0.998.

Given the goodness of this fit, it is natural to wonder whether there is an underlying reason for it. Recht et al. [15] describe a generative model for the data distributions and models that leads to a linear fit in probit domain. Our assumptions are less restrictive and we use them to explain why a good probit fit is likely.

In Figure 4a, the red dashed curve is obtained by mapping the linear fit in probit domain back to probability space. To understand what our analysis says about this phenomenon we also show the guarantees provided by (2) and (10) as the blue and purple curves, respectively, when $\delta_1 = 0.31$, $\delta_2 = 0.38$, $\nu_1 = 0.005$,

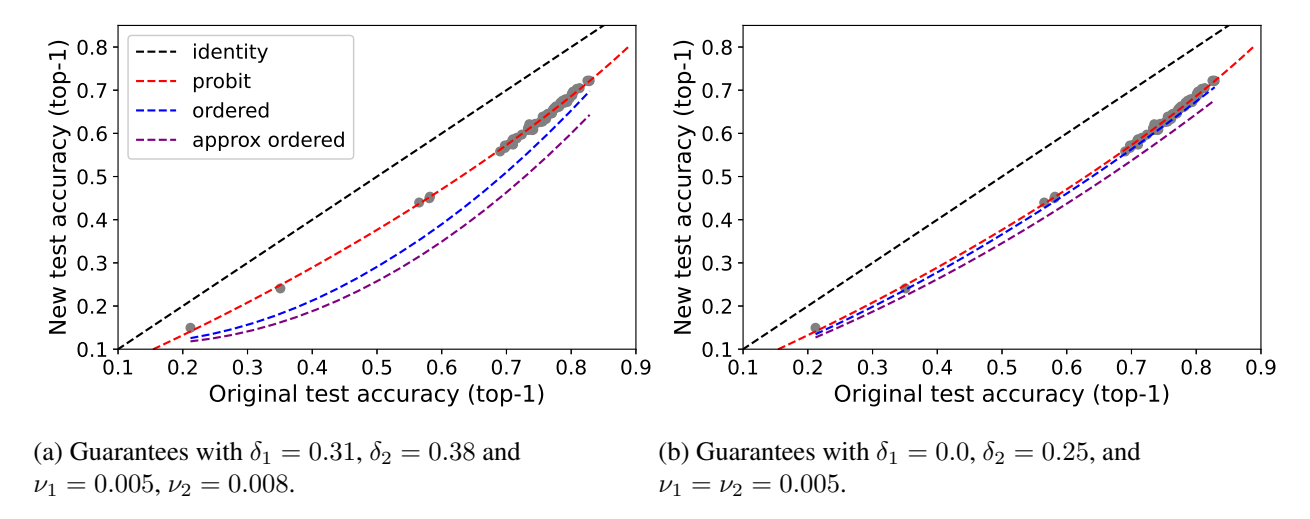


Figure 4: Comparison between probit linear fit of the ImageNet models and our lower bounds.

and $\nu_2 = 0.008$ (values that guarantee that Assumption 1 is satisfied for ImageNetV2 vs ImageNet). The maximal value of (10) is computed numerically by griding, as discussed in Section 5.2. Both the blue and purple curves are lower bounds on test accuracies computed on ImageNetV2. The blue curve assumes the set of models is ordered. On the other hand, the purple curve only assumes the set of models is approximately ordered (we assume the dominance probabilities are at most 0.05).

While the blue and purple curves shown in Figure 4a follow loosely the probit (red) curve, they are not tight lower bounds. However, we can do better. We already discussed that the choice of parameters $\delta_1 = 0.31$, $\delta_2 = 0.38$, $\nu_1 = 0.005$, and $\nu_2 = 0.008$ is conservative. By setting $\delta_1 = 0.$, $\delta_2 = 0.25$, and $\nu_1 = \nu_2 = 0.005$ the constraints of Assumption 1 are satisfied by 95% of the required events. We plot the lower bounds given by (2) and (10) in Figure 4b, as blue and purple curves respectively. Interestingly, the two lower bounds closely follow the probit curve, with the blue and red curves almost overlapping. Therefore, the goodness of the probit linear fit might be a fortuitous consequence of the models saturating the bound shown in (2).

Moreover, we said in Section 2 that when (2) is saturated by f_1 , f_h and some third model f_i , we expect a piecewise linear function to fit the data much better than a simple linear fit. This conclusion can be reached by applying (2) to multiple triplets of models. Given our analysis, we expect a piecewise linear function to better fit the ImageNet models than a linear fit. Indeed, Figure 5 shows a piecewise linear fit with two pieces. The R^2 of this piecewise linear fit is 0.997, which almost identical to the R^2 of the probit linear fit (the difference between the two R^2 scores is 4×10^{-4}). Observing a good piecewise linear fit is likely to be a more general occurrence than a linear fit in probit domain. In fact, [21] saw that a piecewise linear function fits ImageNet models well when they are evaluated on ImageNet-A (a collection of ImageNet test images collected by Hendrycks et al. [10]) and the original ImageNet validation set.

6 Discussion

Given a set of classification models and two data distributions that satisfy two assumptions (both of which can be seen to hold for ImageNetV2 vs ImageNet and CIFAR-10.1 vs CIFAR-10), we showed that the accuracies of the models computed on one distribution are approximately a linear function of the accuracies

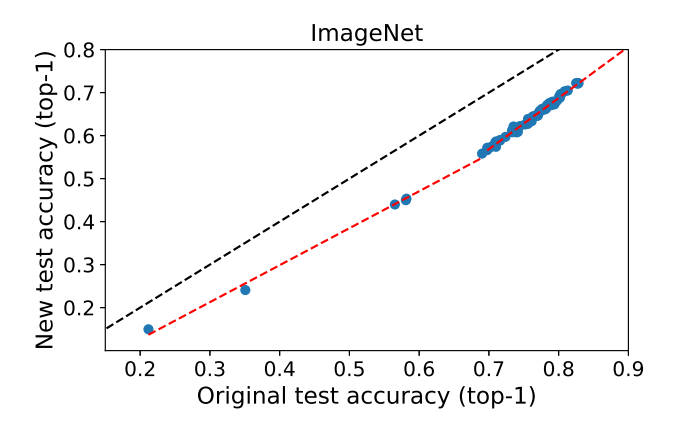


Figure 5: Piecewise linear fit of 66 ImageNet models with two pieces. The switch point between pieces is set to be the 6-th least accurate model.

computed on the other distribution. The crux of our analysis is showing that any three models are approximately collinear, which is achieved by upper bounding the residual from one model to the line defined by the other two models. Moreover, as discussed in Section 5.3, our analysis suggests that in certain regimes a piecewise linear function can better fit the accuracies of the models.

We mentioned that understanding why models are approximately collinear may lead to insights into improving model robustness. According to our analysis, a new model can be more robust than previous models if either it has a higher accuracy than previous models or at least one of our assumptions does not hold. Unsurprisingly, the latter case implies that the new model would have to classify correctly a set of data points that is misclassified by the other models and that has higher probability of occurring under the shifted distribution.

Several open questions remain. We showed that Assumptions 1 and 2 are sufficient to ensure that models are approximately collinear, but it is not clear when we can expect these two assumptions to hold. In particular, Assumption 2 is related to model similarity. It would be interesting to understand what makes models similar. Are models similar due to the data or the model classes we use?

References

- [1] A. Barbu, D. Mayo, J. Alverio, W. Luo, C. Wang, D. Gutfreund, J. Tenenbaum, and B. Katz. Objectnet: A large-scale bias-controlled dataset for pushing the limits of object recognition models. In *Advances in Neural Information Processing Systems*, pages 9453–9463, 2019.
- [2] A. Ben-Tal, D. Den Hertog, A. De Waegenaere, B. Melenberg, and G. Rennen. Robust solutions of optimization problems affected by uncertain probabilities. *Management Science*, 59(2):341–357, 2013.
- [3] E. Delage and Y. Ye. Distributionally robust optimization under moment uncertainty with application to data-driven problems. *Operations research*, 58(3):595–612, 2010.
- [4] J. Deng, W. Dong, R. Socher, L.-J. Li, K. Li, and L. Fei-Fei. Imagenet: A large-scale hierarchical image database. In *2009 IEEE conference on computer vision and pattern recognition*, pages 248–255. Ieee, 2009.

- [5] J. C. Duchi, T. Hashimoto, and H. Namkoong. Distributionally robust losses against mixture covariate shifts. *Under review*, 2019.
- [6] C. Dwork. Differential privacy. In *Proceedings of the International Colloquium on Automata, Languages and Programming (ICALP)*, pages 1–12, 2006.
- [7] C. Dwork, F. McSherry, K. Nissim, and A. Smith. Calibrating noise to sensitivity in private data analysis. In *Theory of cryptography conference*, pages 265–284. Springer, 2006.
- [8] C. Dwork, A. Roth, et al. The algorithmic foundations of differential privacy. *Foundations and Trends in Theoretical Computer Science*, 9(3-4):211–407, 2014.
- [9] P. M. Esfahani and D. Kuhn. Data-driven distributionally robust optimization using the wasserstein metric: Performance guarantees and tractable reformulations. *Mathematical Programming*, 171(1-2): 115–166, 2018.
- [10] D. Hendrycks, K. Zhao, S. Basart, J. Steinhardt, and D. Song. Natural adversarial examples. *arXiv* preprint arXiv:1907.07174, 2019.
- [11] S. Kpotufe and G. Martinet. Marginal singularity, and the benefits of labels in covariate-shift. *arXiv* preprint arXiv:1803.01833, 2018.
- [12] A. Krizhevsky, G. Hinton, et al. Learning multiple layers of features from tiny images. 2009.
- [13] H. Mania, J. Miller, L. Schmidt, M. Hardt, and B. Recht. Model similarity mitigates test set overuse. In *Advances in Neural Information Processing Systems*, pages 9993–10002, 2019.
- [14] J. Miller, K. Krauth, B. Recht, and L. Schmidt. The effect of natural distribution shift on question answering models. *arXiv preprint arXiv:2004.14444*, 2020.
- [15] B. Recht, R. Roelofs, L. Schmidt, and V. Shankar. Do imagenet classifiers generalize to imagenet? *arXiv preprint arXiv:1902.10811*, 2019.
- [16] R. Roelofs, V. Shankar, B. Recht, S. Fridovich-Keil, M. Hardt, J. Miller, and L. Schmidt. A metaanalysis of overfitting in machine learning. In *Advances in Neural Information Processing Systems*, pages 9179–9189, 2019.
- [17] S. Sagawa, P. W. Koh, T. B. Hashimoto, and P. Liang. Distributionally robust neural networks for group shifts: On the importance of regularization for worst-case generalization. *arXiv* preprint *arXiv*:1911.08731, 2019.
- [18] S. Shafieezadeh Abadeh, P. M. Mohajerin Esfahani, and D. Kuhn. Distributionally robust logistic regression. *Advances in Neural Information Processing Systems*, 28:1576–1584, 2015.
- [19] V. Shankar, R. Roelofs, H. Mania, A. Fang, B. Recht, and L. Schmidt. Evaluating machine accuracy on imagenet. In *International Conference on Machine Learning (ICML)*, 2020.
- [20] A. Sinha, H. Namkoong, R. Volpi, and J. Duchi. Certifying some distributional robustness with principled adversarial training. *International Conference on Learning Representations*, 2018.

- [21] R. Taori, A. Dave, V. Shankar, N. Carlini, B. Recht, and L. Schmidt. Measuring robustness to natural distribution shifts in image classification. In *Advances in Neural Information Processing Systems* (NeurIPS), 2020. URL https://arxiv.org/abs/2007.00644.
- [22] C. Yadav and L. Bottou. Cold case: The lost mnist digits. In *Advances in Neural Information Processing Systems*, pages 13443–13452, 2019.

A CIFAR-10.1 vs CIFAR-10

In this section we show that Assumptions 1 and 2 are satisfied by the distributions CIFAR-10.1 and CIFAR-10 and the 30 models we consider.

The blue points shown in Figure 6a represent probabilities of the 274,560 events defined by the triplets $\{f_i, f_j, f_k\}$, as considered in Assumption 1. This empirical evaluation suggests that CIFAR-10 and CIFAR-10.1 satisfy our assumption with $\delta_1 = 0.0$, $\delta_2 = 1.7$, $\nu_1 = 0.005$, and $\nu_2 = 0.02$.

It is important to note that $\delta_2=1.7$ is a large value and if we were to plug it into (6) we would obtain a poor guarantee. However, we remark that the large slop is needed only for events A whose probabilities according to CIFAR-10 are at most 0.03. For events with larger CIFAR-10 probabilities we could use a smaller δ_2 . For example, we could upper bound $\mathbb{Q}(A)$ using $\delta_2=0.8$ and $\nu_2=0.01$ for all events A considered in Assumption 1 that have $\mathbb{P}(A)\geq 0.03$. This choice would ensure that (1) are satisfied for over 95% of events. As discussed in Section 3, our analysis tolerates such refinements.

Figure 6b shows the dominance probabilities of all the pairs of CIFAR-10 models we considers. We note that all these probabilities are smaller than 0.08, with most of them being at most 0.04. Therefore, Assumption 2 is also satisfied with a small ζ .

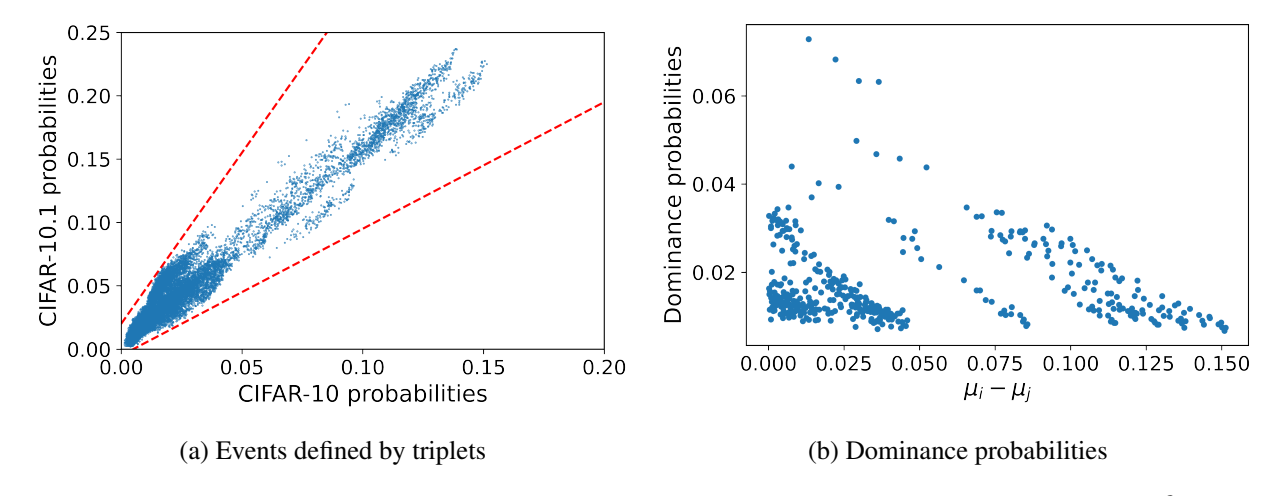


Figure 6: Figure 3a shows 24,360 blue points representing the probabilities of the events $A_i^{\varepsilon_i} \cap A_j^{\varepsilon_j} \cap A_k^{\varepsilon_k}$. The red dotted lines are upper and lower bounds on the probabilities under CIFAR-10.1, as in (1), with parameters: $\delta_1 = 0.0$, $\delta_2 = 1.7$, $\nu_1 = 0.005$, and $\nu_2 = 0.02$. Figure 3b shows the probabilities of the events $A_i^+ \cap A_j^-$ for all pairs of models with $\mu_i < \mu_j$ (i.e., the events on which a worse model is correct, but a better model is incorrect).